



3 1176 00166 6396

DOE/NASA/51044-19  
NASA TM-81771

NASA-TM-81771 19810019985

# Characterization, Performance, and Prediction of a Lead-Acid Battery Under Simulated Electric Vehicle Driving Requirements

John G. Ewashinka and John M. Bozek  
National Aeronautics and Space Administration  
Lewis Research Center

May 1981

LIBRARY COPY

AUG 13 1981

LANGLEY RESEARCH CENTER  
LIBRARY, NASA  
Hampton, Virginia

Prepared for  
**U.S. DEPARTMENT OF ENERGY**  
**Conservation and Renewable Energy**  
**Office of Transportation Programs**

#### **NOTICE**

**This report was prepared to document work sponsored by the United States Government. Neither the United States nor its agent, the United States Department of Energy, nor any Federal employees, nor any of their contractors, subcontractors or their employees, makes any warranty, express or implied, or assumes any legal liability or responsibility for the accuracy, completeness, or usefulness of any information, apparatus, product or process disclosed, or represents that its use would not infringe privately owned rights.**

DOE/NASA/51044-19  
NASA TM-81771

# **Characterization, Performance, and Prediction of a Lead-Acid Battery Under Simulated Electric Vehicle Driving Requirements**

John G. Ewashinka and John M. Bozek  
National Aeronautics and Space Administration  
Lewis Research Center  
Cleveland, Ohio 44135

May 1981

Work performed for  
U.S. DEPARTMENT OF ENERGY  
Conservation and Renewable Energy  
Office of Transportation Programs  
Washington, D.C. 20545  
Under Interagency Agreement DE-AI01-77CS51044

*N81-28523 #*



## SUMMARY

A nominal 6-V state-of-the-art lead-acid battery in current use by the electric vehicle industry as a baseline battery was tested at the NASA Lewis Research Center under laboratory conditions. The primary objective of this work was to determine the effectiveness of regenerative braking in increasing the range of an electric vehicle over the various SAE J227a driving schedules. The current required from an electric vehicle battery depends heavily on the velocity-time profile of the vehicle, the shape and weight of the vehicle, the type of tires used, the efficiency of the propulsion system, the size (voltage) of the battery, and the basic characteristics of the battery (power versus current). Each of these variables is defined in this report with the final resulting current-time profile being representative of the demands placed on a typical state-of-the-art electric vehicle lead-acid battery. The secondary test objective was to obtain the required information on overall battery performance for battery performance modeling.

The velocity-time profiles chosen are defined in the SAE J227a specification, for a hypothetical vehicle with the following characteristics: weight, 1701 kg (3750 lb); product of aerodynamic drag coefficient and projected frontal area  $C_{DA}$ ,  $0.84 \text{ m}^2$  ( $9 \text{ ft}^2$ ); and tire coefficient,  $1.1 \times 10^{-2}$ . The electric vehicle battery pack is a 120-V system consisting of twenty 6-V lead-acid modules. The propulsion system was assumed to have 70 percent efficiency during acceleration and cruise and 50 percent efficiency during regenerative deceleration.

## INTRODUCTION

Many of the performance limitations of an electric vehicle are due to the battery. Not only the cycle life and battery cost but also the range and performance attainable are important. The range of an electric vehicle is also dependent on the type of propulsion system used with the battery. Current propulsion systems under consideration include electrically regenerative and nonregenerative braking systems. Coupled with these two systems are the recuperation effects of the battery and its influence on the performance and range of a vehicle. Another important aspect from the standpoint of the electric vehicle designer is the ability to predict the performance of a lead-acid battery used in an electric vehicle with the propulsion systems mentioned above. This paper addresses the interactions of the propulsion systems with the battery and the prediction of performance and range capability.

Under the sponsorship of the DOE Electric and Hybrid Vehicle Program, the NASA Lewis Research Center has been involved in quantifying the performance of a state-of-the-art lead-acid battery with various electric vehicle propulsion systems. The following are some of the questions that are addressed and discussed in this paper: Does electrically regenerative braking extend the range and performance of an electric vehicle over those of a nonregenerative system? Is there an increase or decrease in range when electrical regeneration is applied to the coast or braking portions of the driving cycles? Can some recuperation extend range when used with a nonregenerative or electrically regenerative propulsion system? What effects on range and performance do other driving schedules have? And finally, can the performance of the battery be predicted with reasonable accuracy for all these situations. Answers to these questions will help in the selection of an optimized electric vehicle propulsion system that not only will be inexpensive but also will be coupled with a battery system that can optimize performance for most driving schedules.

## DETERMINATION OF SAE J227a TESTING PARAMETERS

### Velocity-Time Profile

The power and current required from the battery in an electric vehicle depends heavily on the design of the vehicle and the velocity-time profile over which the vehicle travels. A series of velocity-time profiles are given in SAE J227a (ref. 1). These were used as a basis for calculating the power and current requirements of an electric vehicle battery. The velocity-time profiles chosen are shown in figure 1. The highest vehicle speed for the B schedule is 32.2 km/hr (20 mph); for the C schedule it is 48.3 km/hr (30 mph); and for the D schedule, 72.4 km/hr (45 mph).

### Power Profile at Wheels

To determine the power-time profile for the battery, the power-time profile at the wheels of the vehicle must first be calculated. Once the power-time profile at the wheels is determined, the power-time profile of the vehicle battery can be easily obtained by assuming a propulsion system power efficiency.

The power at the wheels required to move a vehicle can be expressed as

$$\begin{aligned} P_R = & (2.74 \times 10^{-3} TWV + 3.49 \times 10^{-6} TWV^2 + 2.73 \times 10^{-8} TWV^3) \\ & + (1.32 \times 10^{-5} C_D AV^3) + (7.81 \times 10^{-5} WaV) \\ & + (2.42 \times 10^{-3} WV \sin \theta) \end{aligned} \quad (1)$$

The first three terms represent the tire loading (road load). The next terms represent the aerodynamic loads and the acceleration and grade requirements. The tire loading and aerodynamic load terms were obtained from reference 2. The last two terms, acceleration and grade, are self-evident. For equation (1),  $P_R$  in kilowatts is the wheel power,  $T$  is the tire coefficient,  $W$  is the weight of the vehicle in kilograms,  $V$  is the velocity in kilometers per hour,  $C_D$  is the aerodynamic drag coefficient,  $A$  is the projected frontal area in square meters,  $a$  is the acceleration in kilometers per hour per second and  $\theta$  is the grade of the road, in degrees, on which the vehicle is traveling. The grade requirements were not implemented in this report because the power-time requirements of the battery were assumed to be representative of a vehicle operating on a level road. The baseline vehicle was assumed to have the following characteristics:

$$W = 1701 \text{ kg (3750 lbm)}$$

$$C_D = 0.45$$

$$A = 1.86 \text{ m}^2 \text{ (20 ft}^2\text{)}$$

$$T = 0.011$$

To calculate the wheel power, the velocity-time profile of the vehicle must be known. As mentioned earlier, the SAE J227a driving schedules were used. The calculation of wheel power is discussed in three parts. Each part or phase reflects one of the three phases of the velocity-time profiles specified in SAE J227a in which the vehicle is in motion (i.e., acceleration, cruise, and deceleration). The deceleration phase includes the coast and braking periods, which may or may not include electrically regenerative braking.

### Acceleration

During the acceleration phase of the driving schedule it was assumed that the vehicle accelerates at a constant wheel power from 8 km/hr (5 mph) to the cruise speed. Below 8 km/hr, acceleration is constant.

A computer program was developed to determine the wheel power that would meet the acceleration times specified in the SAE J227a driving schedules (fig. 1). The computer program also required that the wheel power at the end of the constant-acceleration portion of the acceleration phase, 8 km/hr (5 mph), match the wheel power during the constant-wheel-power portion of the acceleration phase,  $\geq 8$  km/hr ( $\geq 5$  mph). The resultant wheel power - time requirements are shown in figure 2 for a representative driving schedule (SAE J227a B). The wheel energy from 0 to 8 km/hr (5 mph) is small when compared with the total energy required during the acceleration period. For driving schedules C and D the 0 to 8 km/hr (5 mph) energy requirements are even smaller when compared with the total acceleration energy. Therefore, to facilitate testing, the power required from 8 km/hr (5 mph) to the cruise speed was extended back to 0 km/hr.

The power requirements for the acceleration phase of the SAE J227a driving schedules are given in table I.

### Cruise

The wheel power during the cruise phase can be calculated easily from equation (1). Table II contains the wheel power for the various cruise conditions.

### Deceleration

During the deceleration phase of the driving schedules (coast and braking periods), electrical regeneration may occur. Depending on the design of the vehicle, electrical regeneration may occur during the coast and braking period, just during the braking period, or not at all.

If the vehicle does not have an electrical regeneration capability, the kinetic energy of the vehicle is dissipated totally in the friction brakes and in heating the tires and vehicle skin. If the vehicle is designed such that electrical regeneration occurs during the braking period only, the kinetic energy of the vehicle will be partially dissipated during the coast period. This will result in less energy available for electrical regeneration than when regeneration occurs during the coast and braking periods.

A computer program was developed to determine the wheel power available for electrical regeneration when regeneration occurs during the braking period of the velocity-time profile or during the coast and braking periods of each SAE J227a driving schedule. To facilitate calculations and testing, regenerative wheel power was assumed to be constant. In the computer program the regenerative wheel power was calculated from the differences between the ever-

decreasing kinetic energy of the vehicle as it decelerates and the energy dissipated in heating the vehicle's skin and tires as the vehicle decelerates. The algorithm used in the computer program is given in equation (2).

$$E_k(V_n) - E_k(V_{n+1}) = [P_R(\bar{V}) - P_{reg}] (T_{n+1} - t_n) \quad (2)$$

Here  $E_k(V_n)$  and  $E_k(V_{n+1})$  are the kinetic energies of the vehicle at velocities of  $V_n$  and  $V_{n+1}$ , respectively. The velocity  $V_n$  is the velocity of the vehicle at time  $t_n$ ;  $V_{n+1}$  is the velocity at time  $t_{n+1}$ . The velocity  $V_n$  is always greater than  $V_{n+1}$  since the vehicle is decelerating in the time period  $t_n$  to  $t_{n+1}$ . The term  $P_R(\bar{V})$  represents the wheel power (eq. (1)) at the mean velocity between  $V_n$  and  $V_{n+1}$ , and  $P_{reg}$  is the regeneration wheel power, which is held constant. Equation (2) was reduced to equation (3).

$$T_T = \sum_{t_{initial}}^{t_{final}} (t_{n+1} - t_n) = \sum_{V_{initial}}^{V_{final}} \frac{E_k(V_n) - E_k(V_{n+1})}{P_R(\bar{V}) - P_{reg}} \quad (3)$$

Here  $T_T$  is the time required to decelerate the vehicle from an initial velocity  $V_{initial}$  to the final velocity  $V_{final}$ , usually 0 km/hr. Also  $t_{initial}$  is the time regeneration starts, and  $t_{final}$  is the time regeneration stops. By testing values of  $P_{reg}$  and calculating the resultant  $T_T$ , the proper value of  $P_{reg}$  can be obtained such that the resultant value of  $T_T$  matches the regeneration time specified in the SAE J227a driving schedule.

The results of the computer calculations are given in table III. As expected, the regeneration power at the wheels during the short regeneration period (regeneration during braking period only) was a factor of 2 higher than that during the long regeneration period (regeneration during coast and braking periods). The energy difference was that energy lost in heating the tires and vehicle skin during the coast period.

#### WHEEL POWER SUMMARY

The analysis of the three SAE J227a driving schedules (B, C, and D), when applied to the baseline vehicle, results in the wheel power - time profiles shown in figure 3 and table IV. The negative values in table IV and figure 3 are the regenerative wheel power and energy for a short or long regeneration period.

#### POWER PROFILE AT BATTERY

Once the wheel power was calculated, the battery power was easily obtained by making a few assumptions about the vehicle battery pack design and the propulsion system efficiency.

The propulsion system efficiency was assumed to be 70 percent during acceleration and cruise. It was assumed to drop to 50 percent during regeneration. This drop of 20 percentage points is due to the expected lower efficiency when the propulsion system runs in reverse. Also, in actual driv-



ing conditions some of the vehicle's kinetic energy would be absorbed by the friction brakes acting as a fine control during braking.

The electric vehicle battery was assumed to be a nominal 120-V system. Since only a 6-V battery module was to be tested in the laboratory, an equivalent power profile for the 6-V module would be 1/20th that of the electric vehicle propulsion battery.

Combining the effects of a 70 percent/50 percent efficient propulsion system with the fact that only 1/20th of the vehicle battery pack was to be tested resulted in the power profile to which the 6-V module should be tested, shown in figure 4.

#### CURRENT PROFILES

Since the laboratory facility in which the 6-V module was to be tested could only control current from the battery, the power profiles were transformed into equivalent current profiles.

Before this could be done, a relationship between battery module current and battery module power was required. As discussed later, the relationship was established experimentally. These experiments included (1) discharge characterization tests, a discharge at constant current to a voltage cutoff and (2) charge characterization tests, a controlled current charge (20-sec pulses) at various depth of discharge. As a result of these tests the relationship between power and current was obtained for the 6-V module:

Discharge:

$$P(\text{watts}) = 8.93 I^{0.8963} \quad (4)$$

Charge (regeneration):

$$P(\text{watts}) = 4.34 I^{1.104} \quad (5)$$

From these equations the current-time profiles shown in figure 5 were calculated. It was to those values of current that the 6-V battery was discharged in the laboratory. The two current values during regeneration represent regeneration during the braking period only (short) and regeneration during the coast and braking periods (long).

#### ADDITIONAL CURRENT PROFILES

The previous discussion established the current-time profiles that a 6-V module should experience in the laboratory when simulating the various velocity-time driving schedules. Recent publications (refs. 3 to 5) indicate that the number of profiles possible is a function of rest time. As shown in figure 5, there exist periods where no current is extracted from or regenerated into the battery. To quantify the effects of these rest periods, referred to as recuperation effects, a series of tests were performed. These tests eliminated all rest and regeneration effects. The current-time profiles for these tests are shown in figure 6.

## TESTING PROCEDURE

### Battery Formation

Usually, three to five charge-discharge cycles were required to completely form the battery. Formation is done to stabilize the battery's output capacity in (ampere-hours (AH)). For this battery the rated capacity is 132.5 AH when the battery is discharged at a constant current of 75 A to a battery termination voltage of 5.25 V, or 1.75 V/cell. For the charging portion of the formation cycle a constant-potential method was used with an initial charge current of 20 to 25 A. An overcharge of 10 to 15 percent of the removed capacity was used.

### Discharge Characterization

Discharge characterization tests give the output capacities at various discharge currents to a voltage cutoff. The discharge constant currents used to characterize the test battery were 50, 100, 200, 300, 400, and 500 A, with repeats for each current. The battery was discharged at each current to a voltage cutoff of 3.9 V, or 1.3 V/cell.

### Charge Characterization

This test was an alternate charge and discharge of a battery at a specified depth of discharge (DOD). The charge characterization tests were performed at DOD's of 5, 20, 50, 80, and 100 percent, where DOD is based on the rated capacity of the test battery (132.5 AH). The following was a typical charge characterization test:

Discharged at 75 A to a DOD of 5 percent of rated capacity (6.625 AH),

then charged at 25 A for 20 sec,  
discharged at 75 A for 60 sec,  
charged at 50 A for 20 sec,  
discharged at 75 A for 60 sec,  
charged at 100 A for 20 sec,  
discharged at 75 A for 60 sec,  
charged at 200 A for 20 sec,  
discharged at 75 A for 60 sec,  
charged at 300 A for 20 sec, and  
discharged at 75 A for 60 sec.

The battery was then discharged at 75 A to the next DOD (20 percent, or 26.5 AH) and the above test repeated. These tests were repeated for additional DOD's of 50, 80, and 100 percent of rated battery capacity.

### SAE Driving Cycle Tests

The next three sets of tests were the SAE J227a driving schedules D, C, and B. A schedule consists of five periods that simulate the electric vehicle's acceleration, cruise, coast, braking, and idle periods. Figures 5 and 6 show the three driving schedules and the current levels for each of the five periods.

To quantify the effects of regeneration (long versus short versus none) and the effects of recuperation, four tests were performed on each driving

schedule. In the first test, designated mode "a," the 6-V module was discharged during the acceleration and cruise periods but was allowed to rest during the coast, braking, and idle periods. In the second test, designated mode "b," the module was discharged during the acceleration and cruise periods but was not allowed to rest. A cruise discharge was immediately followed by an acceleration discharge. Comparing test results from mode a to mode b gave a quantitative measure of the effects of recuperation. In the third test, designated mode "c," the 6-V module was discharged during the acceleration and cruise periods, charged during the coast and braking periods (long regeneration), and rested during the idle periods. The fourth test, designated mode "d," is similar to the mode c test except that the module was allowed to rest during the coast and idle periods but was charged during the braking period (short regeneration). Comparing the mode c test results to the mode d test results gave a quantitative measure of the effect of two types of regenerative propulsion system designs (long versus short). Comparing the results of modes c and d to mode a gave a quantitative measure of the effect regeneration has on the performance of an electric vehicle.

The experimental results of driving schedule D modes a, b, c, and d were used to verify mathematical predictions of a vehicle's range with and without regeneration (ref. 6).

#### DESCRIPTION OF FACILITY

The SAE cycling facility at the NASA Lewis Research Center, described in an unpublished paper by R. L. Cataldo of Lewis, was first designed to do simple two-step constant-current cycling discharges. It was later modified for constant-current battery characteristic discharges up to 500 A. Later modifications included the ability for charge characterization tests and SAE J227a driving schedule tests that included regeneration. All these modifications were for constant-current operation. The test facility utilizes a Heuricon programmable sequence timer that has up to 64 programmable time periods. The Heuricon timer with additional circuits controls the charge or discharge periods for the battery under test. The facility includes a 350-A dc power supply for either charge or regeneration and five electronic loads connected in parallel for discharge operation (up to 500 A). Figure 7 shows the SAE cycling facility as it is presently configured.

#### DATA ACQUISITION

The data acquisition for the facility is semiautomatic. Battery specific gravity measurements before and after charge were made with a hydrometer compensated for battery electrolyte temperature. Room temperature and module middle cell temperatures were also recorded before and after tests with a thermometer. The battery terminal voltage and current were recorded continuously on strip-chart recorders. Total ampere-hours accumulated for either charge or discharge were measured with current integrators. A counter was used to record the number of driving cycles completed for a driving schedule test.

## TEST RESULTS AND DISCUSSION

### Discharge Characterization

The discharge characteristic curves for the 6-V module under test are shown in figure 8. All discharges were done at constant current, and the results were plotted with battery terminal voltage as a function of ampere-hours out. The discharge rates were 50, 100, 200, 300, 400, and 500 A constant current. All discharges were terminated at 3.9-V battery terminal voltage. Below 3.9-V, very little capacity can be removed from the module.

Additional information obtained from the discharge characterization tests is presented in table V. For each discharge rate the time and ampere-hour capacity to discharge the battery to 3.9-V is shown. Also shown are the initial and final electrolyte temperatures and specific gravities.

From the data presented in figure 8, another characteristic curve was generated, analogous to a Peukert curve (ref. 7). This curve (fig. 9) gives the discharge time, in minutes, to a specified cutoff voltage, 3.9 or 5.25 V, for discharge current ranging from 50 to 500 A. The data presented in figure 9 are also given in tabular form in table VI. At 75 A to a cutoff voltage of 5.25 V the 6-V module tested was capable of delivering 136 AH, which compares favorably to the module manufacturer's rating of 132.5 AH.

Figure 9 also shows graphically the effect high cutoff voltages had on the length of time the module was able to be discharged. Beyond 200 A the discharge time to the 5.25-V cutoff dropped drastically from that for the 3.9-V cutoff.

The discharge characteristic curves (fig. 8) were also used to calculate the time-averaged power available from the battery at a specific current. The area under each curve in figure 8 for a specific current was measured and the average voltage calculated. By multiplying this voltage by the current, the time-averaged power was calculated for that current. Figure 10 shows the module's time-averaged power as a function of discharge current.

### Charge Characterization

The charge characterization tests described earlier in the report show the effect on the module terminal voltage of various charge rates from 25 to 300 A at various ampere-hour capacities (DOD) (fig. 11). These charge rates are comparable to the regenerative braking rates seen in many electric vehicles. At the low charge rates of 25 to 100 A, battery terminal voltage increased minimally between 13.2 to 132.5 AH removed. However, for charge rates above 200 A battery terminal voltage increased substantially for the same range of ampere-hours removed. At the lower ampere-hour capacities for the 200 A charge rate and above, the battery terminal voltage was between 8.0 and 8.6 V. These higher battery voltages at the high charge rates could cause excessive gassing and/or spewing of electrolyte, shortening the life of the battery. Also, these higher charge rates may promote grid corrosion in the plates, also shortening battery life. With 66.25 AH removed from the battery, or a 50 percent DOD, the battery terminal voltage dropped significantly for the higher charge rates as compared with the lower DOD's (10 percent). Since the charge rates (25 to 300 A) are comparable to the regenerative braking rates seen in many electric vehicles, the high current regeneration for an electric vehicle application should only be permitted after 50 percent of its capacity has been removed. Regeneration can be used at the lower charge rates, below 100 A, at any DOD.

## SAE J227a Tests

The relationship between charge rate in amperes and power in watts was obtained by a regression analysis of all available data gathered in the charge characterization tests. Although the power at a specific charge rate depends on the DOD (voltage variations with DOD in fig. 11), the spread was judged to be small. The resultant power versus charge current is given in figure 12.

As mentioned previously in this report, three driving schedules with four modes of operation within each schedule were tested. Table VII gives representative data for all schedules and modes and includes the time and ampere-hours removed to a terminal voltage of 3.9 V. Also given in table VII are the initial and final electrolyte temperatures, the initial and final average specific gravities, and the number of profiles completed. For all schedules the number of profiles completed was greater when regeneration was used than when the nonregenerative modes (a and b) were used. Also, more profiles were completed for all schedules that had acceleration, cruise, and rest than with the acceleration and cruise profile (mode a versus mode b). Obviously, mode b operation within each SAE J227a driving schedule is the worst case, giving lower profiles than mode a, c, or d. There seems to be little difference between modes c and d for all schedules as far as the number of profiles completed (long versus short regeneration). Therefore regeneration can occur during braking only or during braking and coast without influencing the number of completed profiles. Table VIII summarizes all the driving cycle tests. Included in this table are the number of tests, the number of profiles completed, the average number of profiles completed, and the equivalent range.

The reproducibility of the tests was judged to be excellent. The maximum deviation was  $\pm 3.4$  percent, which occurred during the most stressful tests (i.e., the SAE J227a driving schedule D with high current regeneration during the braking period (short regeneration period, mode d)). The table shows no substantial difference between the range of an electric vehicle with a propulsion system designed to regenerate during the braking period only (short) and a propulsion system permitting regeneration during the coast and braking periods (long). All mode c and mode d tests resulted in ranges that were equal within experimental error.

An electric vehicle having a propulsion system allowing regeneration was shown to have a range substantially greater than one not having regeneration. The average range for the regenerative tests (mode c and mode d tests) when compared with the nonregenerative tests (mode a) showed a 12.5 percent increase in range due to regeneration for the D driving schedule. For the C and B driving schedules the range increases were 20.1 and 24.7 percent, respectively. The difference in the percentage of range increase between the D driving schedule and the C and B driving schedules is primarily due to (1) the amount of capacity returned to the battery during regeneration as compared with the capacity removed during the acceleration and cruise phases of the profile and (2) the number of stops per kilometer traveled. The D driving schedule returned about 8 percent of the discharged capacity per profile; the C and B driving schedules returned about 14 percent (refer to table VII). The D driving schedule has 0.62 stop/km (1 stop/mile); the C driving schedule has 1.7 stops/km (2.7 stops/mile), and the B driving schedule has 2.9 stops/km (4.5 stops/mile). Therefore the C and B driving schedules returned a higher percentage of capacity removed from the battery per unit distance traveled than did the D driving schedule.

Recuperation of the battery during rest periods will increase the range of an electric vehicle. All mode a tests that had a rest phase during the

coast, braking, and idle periods resulted in a greater electric vehicle range than all mode b tests. The SAE J227a D driving schedule test had a 10.1 percent increase in range with recuperation over the range measured without recuperation. The C and B driving schedules had 12.0 and 5.4 percent increases, respectively. The substantially lower increase for the B driving schedule was probably due to the low recuperation period of 34 sec as compared with 44 and 42 sec for the D and C driving schedules. Recuperation effects were also expected to be reduced when the discharge levels prior to rest periods were low. The time-averaged current during the acceleration and cruise periods of the driving schedule were 153.7, 90.6, and 40.0 A for the SAE J227a D, C, and B driving schedules, respectively.

Figure 13 shows the battery terminal voltage as a function of the number of profiles for the four test modes of SAE J227a driving schedule D. All tests were terminated when the battery voltage reached 3.9 V. In all cases the tests were terminated during the acceleration portion of the profile. The data presented in figure 13 were used to verify the mathematical model proposed in the latter part of this report.

### Battery Model Predictions

The averaging battery model, fully explained in reference 3, was used to predict the performance limits of the lead-acid battery module tested. The algorithm of the averaging battery model, in its simplest form, is equation (6) (eq. (8) in ref. 3).

$$\text{Number of profiles} = \frac{C}{(AH_D)/\text{profile} - (AH_R)/\text{profile}} \quad (6)$$

where C is the capacity available from the battery at the time-averaged discharge current. The denominator of the equation is the discharge capacity removed per profile  $(AH_D)/\text{profile}$  and the capacity returned to the battery during regeneration per profile  $(AH_R)/\text{profile}$ . The model as described in reference 3 has been expanded in this report to include not only a prediction of the number of SAE J227a driving profiles possible, but also a prediction of the voltage of the battery as the discharge progresses. The discussion that follows is divided accordingly.

### Profile Predictions

Table IX gives the results of applying the averaging battery model and a comparison with the laboratory tests reported earlier in this report. Columns 1 and 2 in table IX give the SAE J227a driving schedules and their associated modes. Column 3 gives the average number of discharge profile completed in the laboratory test (table VIII). Columns 4 and 5 show the design capacity removed per profile and the design capacity per profile returned to the module during regeneration. Column 7 gives the calculated time-averaged discharge current. This current was obtained by simply dividing the values in column 4 by the time required to complete one profile, column 6. The net capacity available, column 8, was calculated from the current-capacity relationship presented in figure 14. The experimental data for the current-capacity relationships, obtained from table V, were fitted to a curve with the following equation:

$$C = 309.87 - 39.29 \ln I \quad (7)$$

where C is the capacity in ampere-hours possible at a current I in amperes. By applying equation (7) to the time-averaged current in column 7, the capacity available C was calculated. Column 9 presents the number of profiles possible for the various SAE J227a driving schedules calculated from equation (6). Column 10 presents the percentage deviation between the calculated and experimental results.

As can be seen in table IX, a deviation of nearly 10 percent occurs only for SAE J227a driving schedule B. Unfortunately the average current for this profile is substantially less than the lowest experimental current in the discharge characterization tests, which was used to generate equation (7). Therefore an extrapolation was used to calculate the net capacity available, which could be in error.

#### Voltage Predictions

The basic theses on which the calculation of battery voltage is based are

(1) Battery discharge voltage depends on the instantaneous discharge rate and the state of charge of the battery at the time of interest.

(2) Battery charge voltage (i.e., regenerative voltage) depends on the instantaneous charge rate and the capacity removed at the time of interest. The state of charge of a battery is defined as

$$F_I(t) = \frac{\int_0^n i_D dt - \int_0^t i_R dt}{C} \quad (8)$$

Here  $F_I(t)$  is the state of charge at time t,  $i_D$  is the discharge current,  $i_R$  is the regeneration current, and C is the capacity available at the time-averaged current. This is a restatement of the state of charge defined in reference 3 (eq. (6)) assuming a regenerative effectiveness of 1.

From this definition of state of charge, the data presented in figure 8 were replotted in figure 15 as a function of state of charge. Here zero-percent state of charge is the capacity removed to a cutoff voltage of 3.9 V at a specific current. Other states of charge at that current are the ratio of the capacity removed to the capacity at zero-percent state of charge. For example, at 50 A the battery delivers 152 AH to 3.9 V. At 100 AH removed, the state of charge is 100/152, or 65.8 percent. Therefore the voltage of the battery at 65.8 percent state of charge is 5.9 V.

To demonstrate the efficacy of the two basic theses, the SAE J227a driving schedule D laboratory tests were analyzed and the predicted voltages compared with the experimental voltages. The two theses require data of current versus voltage versus state of charge for constant-current discharges and data on the voltage at a specific charge current and capacity removed at the time charge occurs. The D driving schedule tests have two levels of discharge, 234 and 109 A, and two levels of regeneration, 54 and 96 A. The experimental data in figures 15 and 11 are replotted for these currents and presented in figures 16 and 17 for discharge and charge (regeneration), respectively.

A calculator was programmed to determine the state of charge and capacity removed as a function of the number of D profiles completed. The calculated and experimental voltages are compared in figure 18. The data points are calculated values; the continuous curves are experimental data.

As can be seen, for schedule D, modes a and b (figs. 21 and 22, respectively), there is good agreement between calculated and experimental data. For schedule D, modes c and d (figs. 18(c) and (d), respectively), the agree-

ment is less desirable but judged to be adequate. The error in these last two tests is no greater than 0.25 V out of about 6 V, or 4 percent. Much of this error may be attributed to the experimental variation of battery voltage during the discharge characterization tests.

## CONCLUSIONS

### Charge Characterization

Charge (regeneration) has the effect of increasing the battery terminal voltage at any depth of discharge (DOD). At the lower charge (regeneration) rates of between 25 to 100 A, a small increase in battery voltage results between DOD's of 10 to 100 percent. However, for charge (regeneration) currents above 100 A the battery terminal voltage is substantially increased. These higher battery voltages at the higher charge rates could affect battery life and performance by causing corrosion of the battery plate grids. Also, these higher rates may cause spewing of the electrolyte from the battery vent caps. Excessive gassing can also occur, requiring more water than normal. A general conclusion from these tests is that the regeneration rate should be at 100 A or lower at all DOD's.

### Driving Schedule Tests

For all SAE J227a driving schedules, both regeneration and recuperation increase the range of an electric vehicle. For the D driving schedule the increase due to regeneration (average of the long and short regeneration) was 12.5 percent. For the C driving schedule it was 20.1 percent, and for the B driving schedule it was 24.7 percent. For the D driving schedule the increase due to recuperation was 10.1 percent. For the C schedule it is 12.0 percent, and for the B driving schedule it was 5.4 percent.

The laboratory test data indicate that regeneration during the driving profile's coast and braking periods or during the braking period alone has little effect on the number of profiles completed. In all SAE J227a driving schedules the number of profiles completed for long and short regeneration periods were equal within experimental reproducibility.

### Model Predictions

The time-averaging battery performance model has successfully predicted the performance, both performance limit and voltage, of a lead-acid battery. When the lead-acid battery was subjected, in the laboratory, to the demands approximating an electric vehicle driven of the various SAE J227a driving schedules, the model predicted the performance limit within +2.4 percent to -3.7 percent for the D schedule, +0.5 to -7.1 percent for the C schedule, and better than -11.4 percent for the B schedule. The time-averaging battery performance model was also able to predict the battery voltage, during the acceleration, cruise, and regeneration periods of the driving schedules, to within 250 mV (4 percent) of the experimental values.



## REFERENCES

1. Electric Vehicle Test Procedure. SAE Recommended Practice J227a, SAE Handbook, Society of Automotive Engineers, Inc., 1979, pp. 27.07 - 27.12.
2. Salihi, Jalal T.: Energy Requirements for Electric Cars and Their Impact on Electric Power Generation and Distribution Systems. IEEE Trans. Ind. Appl. vol. IA-9, no. 5, Sept./Oct. 1973, pp. 516-532.
3. Bozek, John M.: An Averaging Battery Model for a Lead-Acid Battery Operating in an Electric Car. DOE/NASA/1044-79/5, NASA TM-79321, 1979.
4. Welz, J. J.: Some Aspects of Battery Vehicle Evaluation with Particular Attention to a Battery Model. Presented at the Third International Electric Vehicle Exposition and Conference, St. Louis, Mo., May 20-22, 1980.
5. Martin, H. Lee: New Concepts in Battery Performance Simulation and Monitoring. Presented at the Third International Electric Vehicle Exposition and Conference, St. Louis, Mo., May 20-22, 1980.
6. Bozek, John M.: An Electric Vehicle Propulsion System's Impact on Battery Performance - An Overview. Presented at the Third International Electric Vehicle Exposition and Conference, St. Louis, Mo., May 20-22, 1980.
7. Peukert, W.: Ueber die Abhängigkeit der Kapazität von de Entaldestromstärke bei Bleiakumulatoren. Elektrotech. Z., Heft 20, May 20, 1897, pp. 287-288.

TABLE I. - ACCELERATION WHEEL POWER

SAE J227a driving schedule	Acceleration specifications	Wheel power, kW
B	0 to 32.2 km/hr (20 mph) in 19 sec	4.7
C	0 to 48.3 km/hr (30 mph) in 18 sec	10.4
D	0 to 72.4 km/hr (90 mph) in 28 sec	16.6

TABLE II. - CRUISE WHEEL POWER

SAE J227a driving schedule	Cruise specifications		Wheel power, kW
	km/hr	mph	
B	32.2	20	2.1
C	48.3	30	3.9
D	72.4	45	8.4

TABLE III. - REGENERATIVE BRAKING

WHEEL POWER AND ENERGY

SAE J227a driving schedule	Regeneration wheel power, kW	Regeneration wheel energy,	
		kJ	kW-hr
B	<sup>a</sup> 6.4	58	0.016
	<sup>b</sup> 10.9	54	.015
C	<sup>a</sup> 6.9	112	.031
	<sup>b</sup> 12.0	97	.027
D	<sup>a</sup> 14.1	266	.074
	<sup>b</sup> 26.7	241	.067

<sup>a</sup>Electrical regeneration occurs during coast and braking periods of driving schedule (long).

<sup>b</sup>Electrical regeneration occurs only during braking period (short).

TABLE IV. - WHEEL POWER REQUIRED FOR SAE J227a

DRIVING SCHEDULES

SAE J227a driving schedule	Driving phase <sup>a</sup>	Elapsed time, sec	Power, kW	Energy,	
				kJ	kW-hr
B	Acceleration	0 to 19	4.7	90	0.025
	Cruise	19 to 38	2.1	40	.011
	Long regeneration	38 to 47	-6.4	-58	-.016
	Short regeneration	42 to 47	-10.9	-54	-.015
C	Acceleration	0 to 18	10.4	187	0.052
	Cruise	18 to 38	3.9	79	.022
	Long regeneration	38 to 54	-6.9	-112	-.031
	Short regeneration	46 to 54	-12.0	-97	-.027
D	Acceleration	0 to 28	16.6	464	0.129
	Cruise	28 to 78	8.4	421	.117
	Long regeneration	78 to 97	-14.1	-266	-.074
	Short regeneration	88 to 97	-26.7	-241	-.067

<sup>a</sup>Refer to table III for definitions of long and short regeneration.

TABLE V. - DISCHARGE CHARACTERIZATION

Test	Mode	Discharge time, min	Ampere-hour capacity to discharge, <sup>a</sup> AH	Temperature, °C		Specific gravity (average)	
				Initial	Final	Initial	Final
1	50-A discharge	182.4	151.8	24	25	1.281	1.130
2	100-A discharge	77.6	129.2	26	29	1.284	1.164
3	200-A discharge	30.5	101.5	24	31	1.286	1.193
4	300-A discharge	16.9	84.8	23	33	1.284	1.209
5	400-A discharge	11.4	74.8	22	35	1.279	1.209
6	500-A discharge	8.1	67.6	24	40	1.284	1.226

<sup>a</sup>To 3.9 V battery terminal voltage.

TABLE VI. - PEUKERT CURVE DATA

Current, A	Voltage cutoff, V	
	5.25	3.9
	Time, min	
50	165.6	182.4
100	71.4	77.6
200	24.6	30.5
300	5.0	16.9
400	.22	11.4
500	.06	8.1

TABLE VII. - SAE J227a DRIVING SCHEDULE TEST RESULTS

SAE J227a driving schedule	Mode	Total discharge, time, min	Temperature, °C		Ampere-hour capacity		Specific gravity		Number of profiles completed	Range*	
			Initial	Final	Removed	Regenerated	Initial	Final		km	miles
D	a	77.3	23	29	126.8	0	1.284	1.161	38	<sup>a</sup> 65	40.3
	b	46.8	25	34	115.5	0	1.283	1.170	34	<sup>b</sup> 58.1	36.0
	c	87.4	27	39	145.2	12.3	1.296	1.169	43	<sup>c</sup> 73.5	45.6
	d	85.4	23	34	138.1	10.1	1.297	1.169	42	<sup>d</sup> 71.8	44.5
C	a	213.3	23.5	30.5	156.3	0	1.296	1.130	162	<sup>e</sup> 97.2	59.9
	b	93.7	24	31.5	143.3	0	1.296	1.146	148	<sup>f</sup> 88.8	54.8
	c	264.6	24.5	34	175.2	25.13	1.296	1.130	201	<sup>g</sup> 121	74.4
	d	268.6	27	34	177.1	21.0	1.304	1.130	204	<sup>h</sup> 122	75.5
B	a	549.6	23	27	199.4	0	1.307	1.130	458	<sup>i</sup> 160	100.8
	b	276.8	24	28	188.8	0	1.307	1.130	437	<sup>j</sup> 153	96.1
	c	682.8	25	29	208.1	35.28	1.309	1.130	569	<sup>k</sup> 199	125.2
	d	678.0	24	29	209.8	33.34	1.311	1.130	565	<sup>l</sup> 197	124.3

<sup>a</sup>72-km/hr top speed - no regeneration with recuperation during coast, braking, and idle periods.  
<sup>b</sup>72-km/hr top speed - no regeneration and no recuperation.  
<sup>c</sup>72-km/hr top speed - regeneration during braking and coast periods with recuperation during idle periods.  
<sup>d</sup>72-km/hr top speed - regeneration during braking periods with recuperation during coast and idle periods.  
<sup>e</sup>48-km/hr top speed - no regeneration with recuperation during coast, braking, and idle periods.  
<sup>f</sup>48-km/hr top speed - no regeneration and no recuperation.  
<sup>g</sup>48-km/hr top speed - regeneration during braking and coast periods with recuperation during idle periods.  
<sup>h</sup>48-km/hr top speed - regeneration during braking periods with recuperation during coast and idle periods.  
<sup>i</sup>32-km/hr top speed - no regeneration with recuperation during coast, braking, and idle periods.  
<sup>j</sup>32-km/hr top speed - no regeneration and no recuperation.  
<sup>k</sup>32-km/hr top speed - regeneration during braking and coast periods with recuperation during idle periods.  
<sup>l</sup>32-km/hr top speed - regeneration during braking periods with recuperation during coast and idle periods.  
 \*Based on 0.35 km (0.22 mile) per B schedule; 0.60 km (0.37 mile) per C schedule; 1.71 km (1.06 mile) per D schedule.

TABLE VIII. - SUMMARY OF ALL DRIVING SCHEDULE TESTS

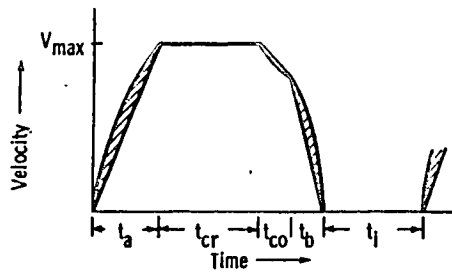
SAE J227a driving schedule	Mode	Number of tests	Number of profiles completed	Average number of profiles completed + percent	Range <sup>a</sup> + percent	
					km	miles
D	a	3 ↓	38, 38, 38	38+0	65.0+0	40.3+0
	b		35, 34	34.5+1.4	59.0+1.4	36.6+1.4
	c		43, 41	42+2.3	71.8+2.3	44.5+2.3
	d		45, 42	43.5+3.4	74.4+3.9	46.1+3.4
C	a	3 ↓	162, 173	167.5+3.3	101+3.3	62.0+3.3
	b		148, 151	149.5+1.0	89.7+1.0	55.3+1.0
	c		201, 207	204+1.5	122+1.5	74.5+1.5
	d		204, 193	198.5+2.8	119.1+2.8	73.4+2.8
B	a	3 ↓	458, 472	465+1.5	163+1.5	102+1.5
	b		437, 445	441+1.0	154+1.0	97.0+1.0
	c		569, 594	581+2.1	203+2.1	128+2.1
	d		565, 593	579+2.4	203+2.4	127+2.4

<sup>a</sup>See table VII notes.

TABLE IX. - COMPARISON OF CALCULATED AND EXPERIMENTAL SAE J227a BATTERY PERFORMANCE

SAE J227a driving schedule	Mode	Average number of laboratory profiles completed	Gross discharge capacity per profile, AH	Regeneration capacity per profile, AH	Time per profile, sec	Time-averaged current, A	Calculated net capacity per discharge, AH	Calculated profiles possible	Deviation, percent
D	aa	38+0	3.33 ↓	-----	122	98.3	129.6	38.9	+2.4
	bb	34.5+1.4		-----	78	153.7	112.0	33.6	-2.6
	cc	42+2.3		0.285	122	98.3	129.6	42.6	+1.4
	dd	43.5+3.4		.240	122	98.3	129.6	41.9	-3.7
C	ae	167.5+3.3	0.956 ↓	-----	78	44.1	161.1	168.5	+0.5
	bf	149.5+1.0		-----	38	90.6	132.8	138.9	-7.1
	cg	204+1.5		0.124	78	44.1	161.1	193.6	-5.1
	dh	198.5+2.8		.102	78	44.1	161.1	188.6	-5.0
B	ai	465+1.5	0.422 ↓	-----	72	21.1	190.1	450.5	-3.1
	bj	441+1.5		-----	38	40.0	164.9	390.8	-11.4
	ck	581+2.1		0.0625	72	21.1	190.1	528.8	-9.1
	dl	579+2.4		.0597	72	21.1	190.1	523.8	-9.5

- a72-km/hr top speed - no regeneration with recuperation during coast, braking, and idle periods.
- b72-km/hr top speed - no regeneration and no recuperation.
- c72-km/hr top speed - regeneration during braking and coast periods with recuperation during idle periods.
- d72-km/hr top speed - regeneration during braking periods with recuperation during coast and idle periods.
- e48-km/hr top speed - no regeneration with recuperation during coast, braking, and idle periods.
- f48-km/hr top speed - no regeneration and no recuperation.
- g48-km/hr top speed - regeneration during braking and coast periods with recuperation during idle periods.
- h48-km/hr top speed - regeneration during braking periods with recuperation during coast and idle periods.
- i32-km/hr top speed - no regeneration with recuperation during coast, braking, and idle periods.
- j32-km/hr top speed - no regeneration and no recuperation.
- k32-km/hr top speed - regeneration during braking and coast periods with recuperation during idle periods.
- l32-km/hr top speed - regeneration during braking periods with recuperation during coast and idle periods.



Part of driving cycle	SAE J227a schedule		
	B	C	D
	Maximum velocity, $V_{max}$		
	$32 \pm 1.5$ km/hr ( $20 \pm 1$ mph)	$48 \pm 1.5$ km/hr ( $30 \pm 1$ mph)	$72 \pm 1.5$ km/hr ( $45 \pm 1$ mph)
Time, sec			
$t_a$ - acceleration	$19 \pm 1$	$13 \pm 2$	$28 \pm 2$
$t_{cr}$ - cruise	$19 \pm 1$	$20 \pm 1$	$50 \pm 2$
$t_{co}$ - coast	$4 \pm 1$	$8 \pm 1$	$10 \pm 1$
$t_b$ - braking	$5 \pm 1$	$9 \pm 1$	$9 \pm 1$
$t_i$ - idle	$25 \pm 2$	$25 \pm 2$	$28 \pm 2$
Total	$72 \pm 2$	$80 \pm 2$	$122 \pm 2$

Figure 1. - SAE J227a velocity-time profiles.

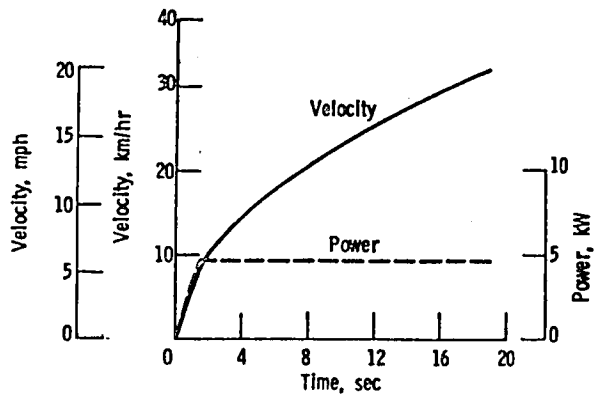
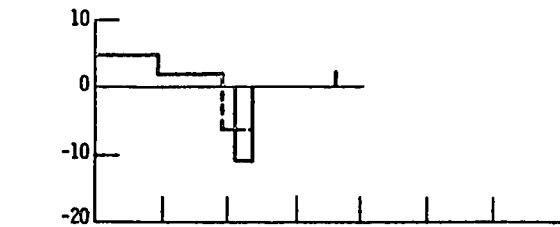
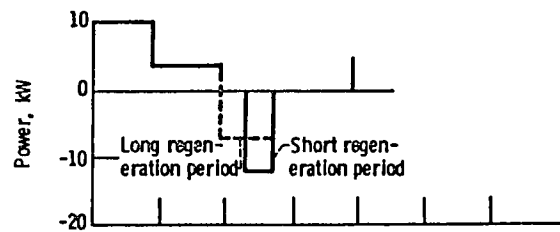


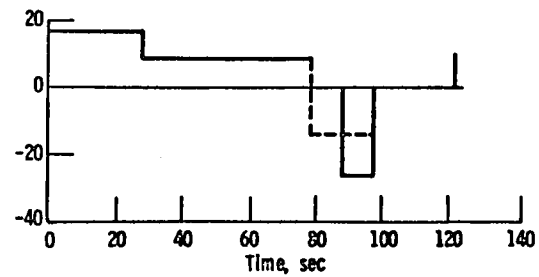
Figure 2. - SAE J227a acceleration profile.



(a) Schedule B.



(b) Schedule C.



(c) Schedule D.

Figure 3. - Wheel power required for SAE J227a driving schedules.

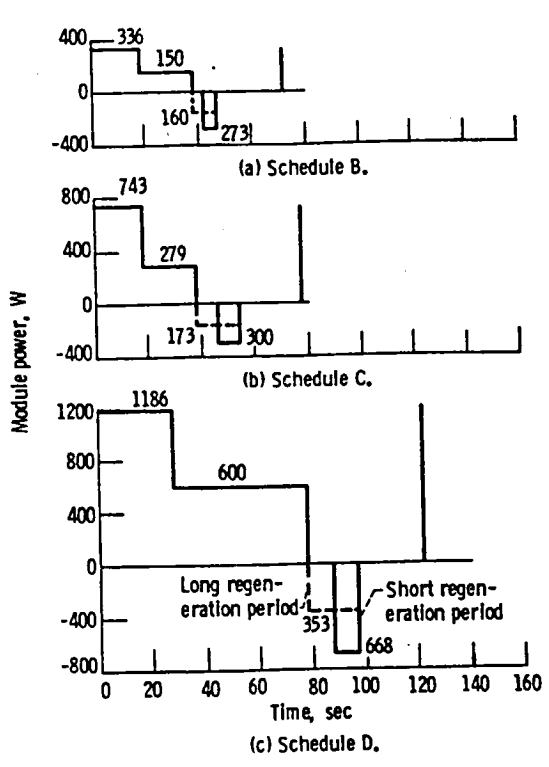


Figure 4. - Power profiles for 6-V module test.

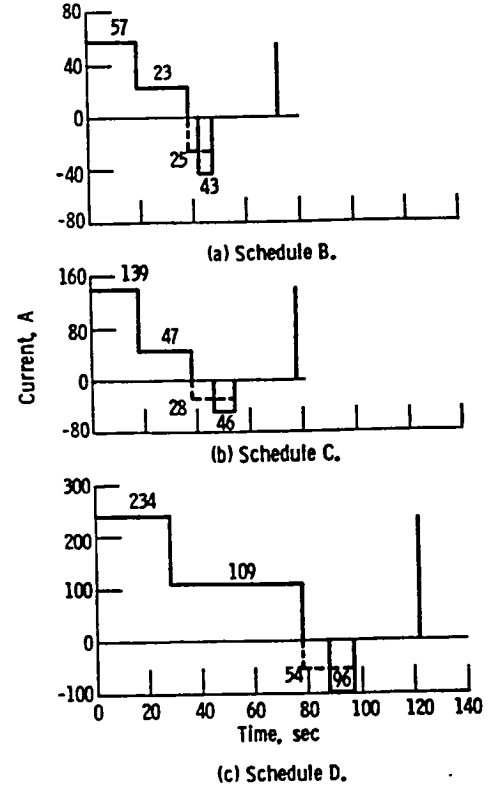


Figure 5. - Discharge current profiles showing rest periods.

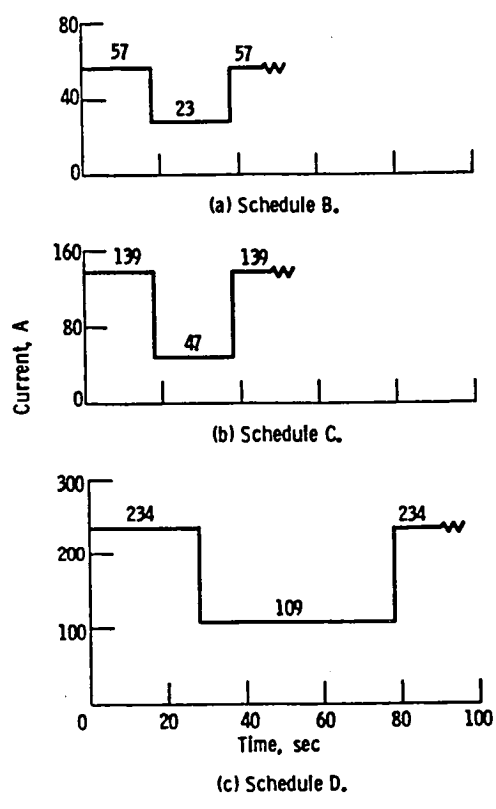


Figure 6. - Discharge current profiles for showing recuperation effects.

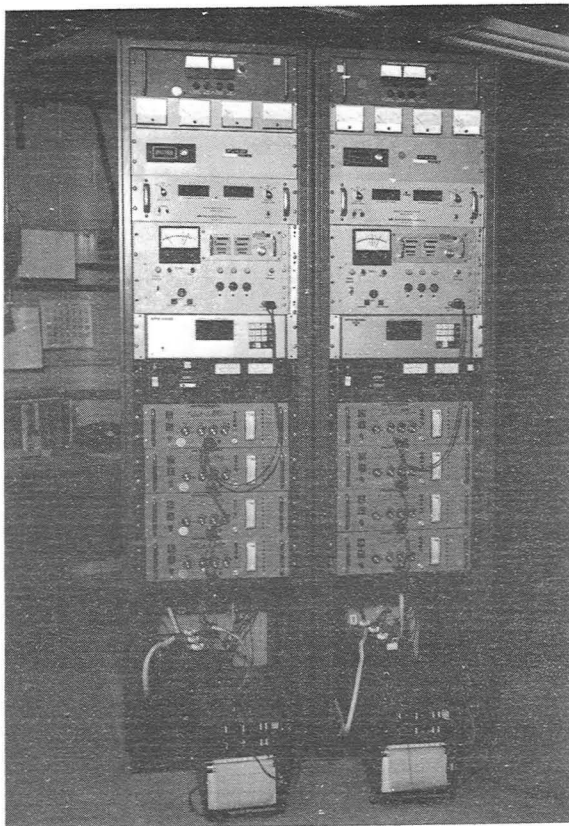


Figure 7. - SAE cycling facility.

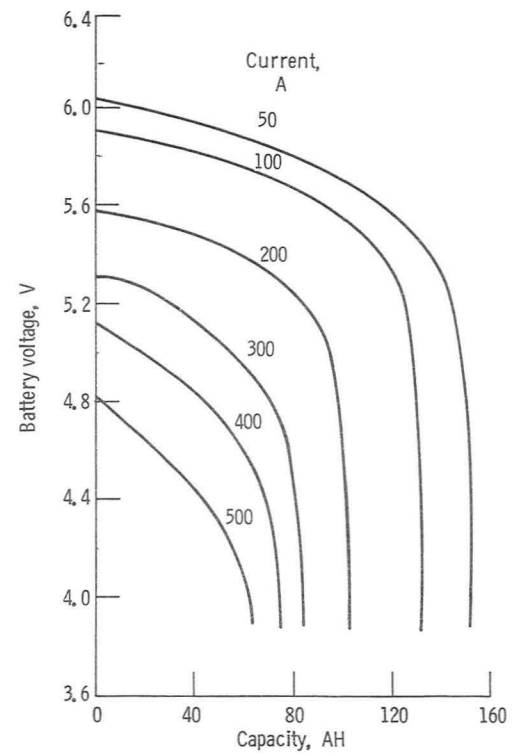


Figure 8. - Discharge characterization.



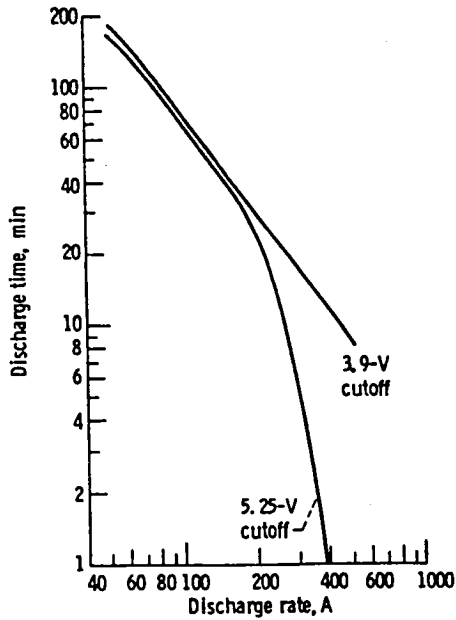


Figure 9. - Peukert curve.

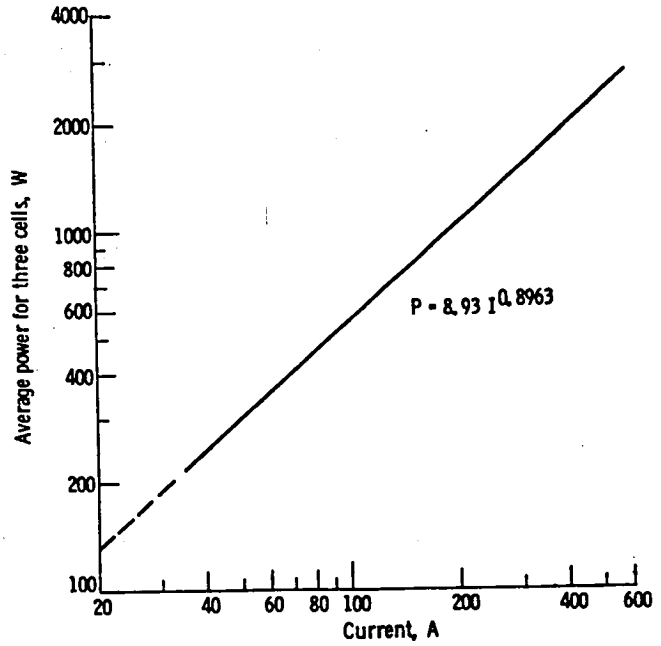


Figure 10. - Module time-averaged power as a function of discharge current.

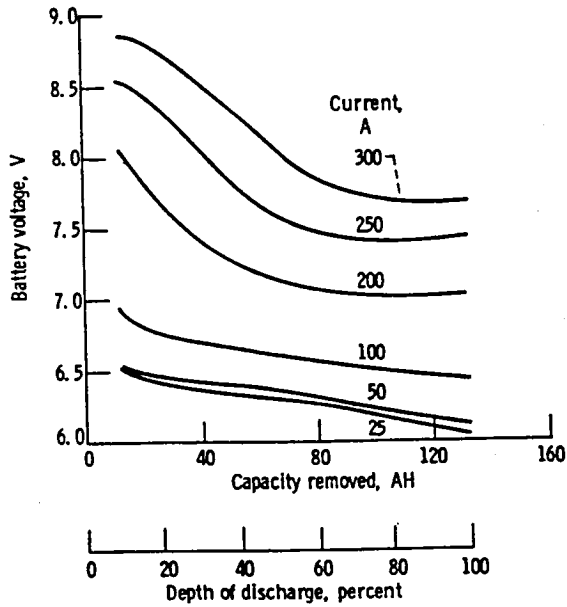


Figure 11. - Charge characterization of three-cell battery after 20-sec charge pulse. (DOD is based on 132.5 AH removed at 75 A to 5.25 V per battery.)

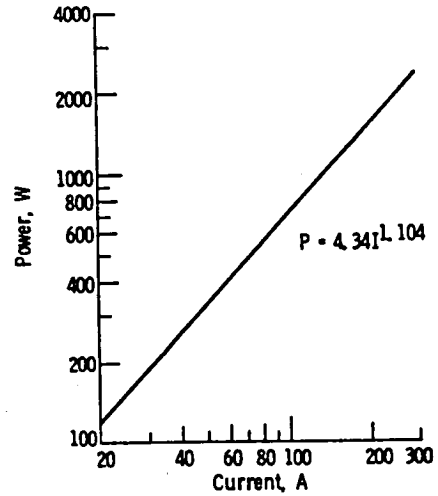


Figure 12. - Charge characterization (current versus power).

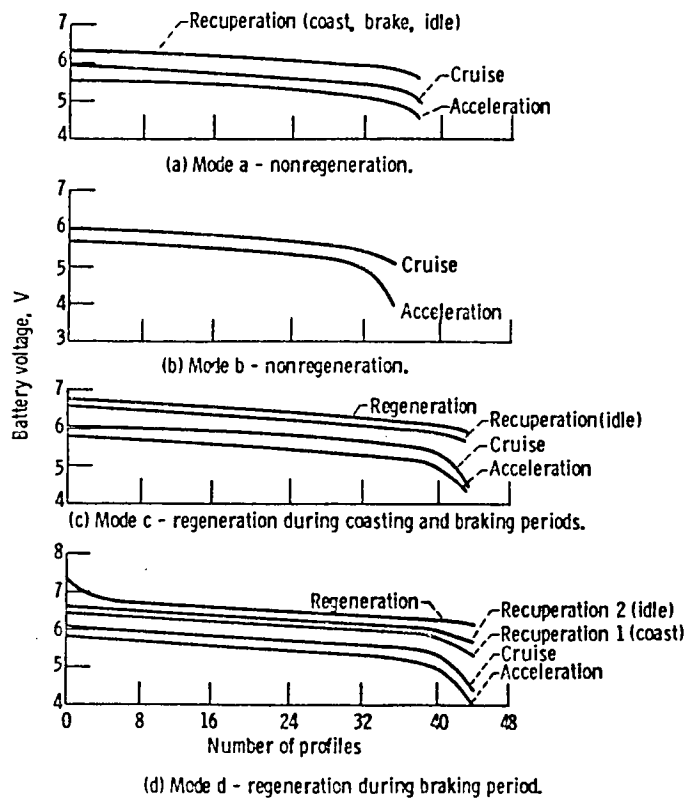


Figure 13. - SAE driving schedule D.

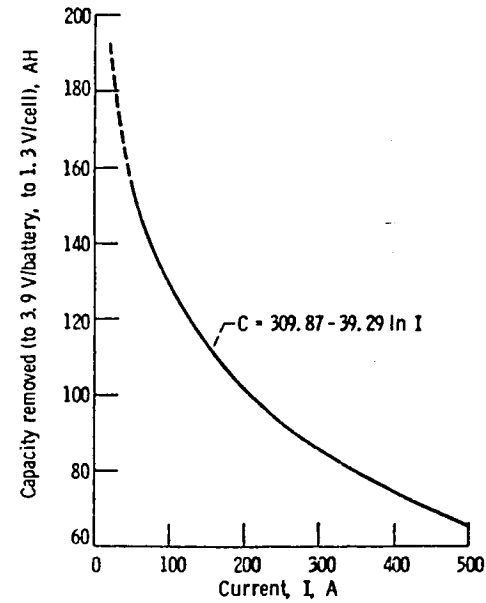


Figure 14. - Measured current - capacity relationship.

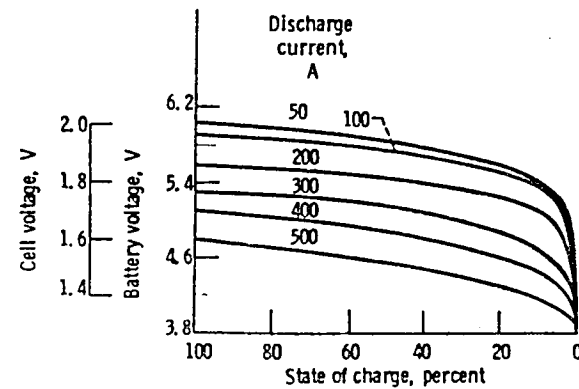


Figure 15. - Discharge characterization on current basis.

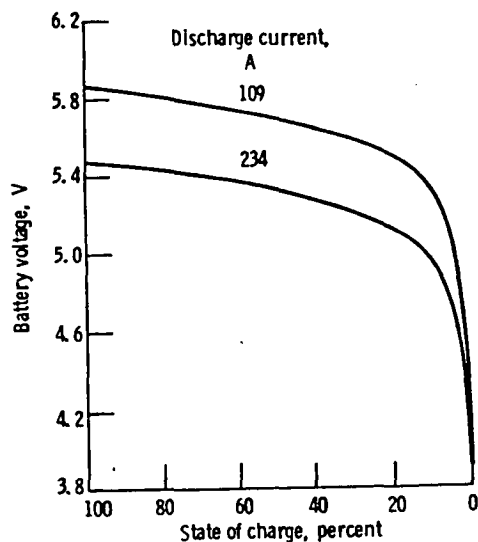


Figure 16. - Discharge characterization as a function of state of charge.

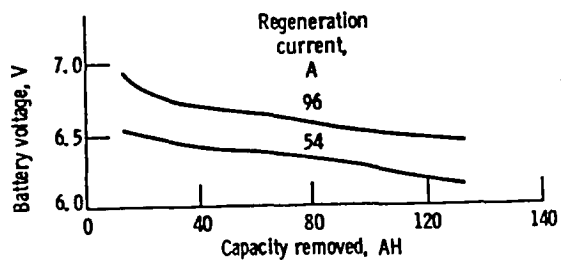


Figure 17. - Charge characterization as a function of capacity removed from battery.

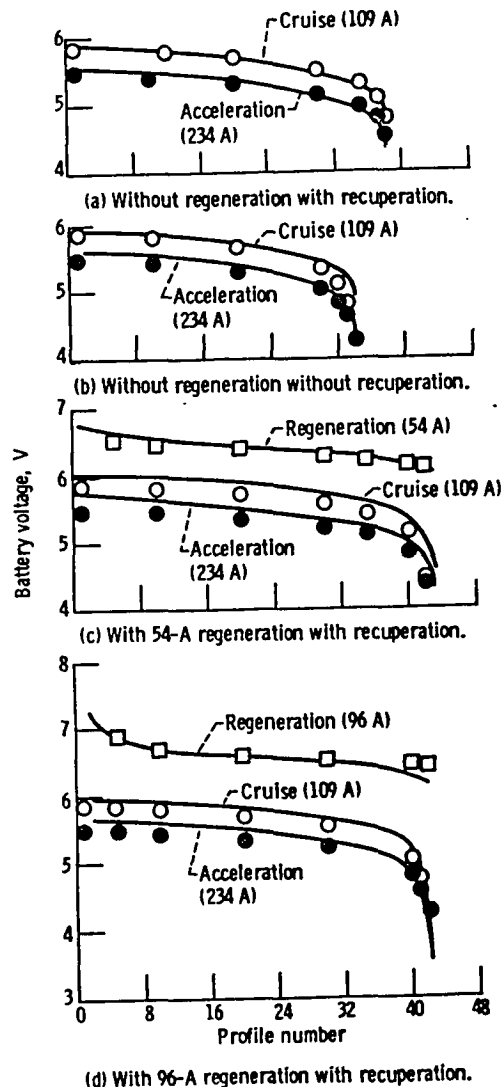


Figure 18. - State of charge and capacity removed as a function of number of profiles completed for SAE J227a schedule D.

1. Report No. NASA TM-81771		2. Government Accession No.		3. Recipient's Catalog No.	
4. Title and Subtitle CHARACTERIZATION PERFORMANCE AND PRE- DICTION OF A LEAD ACID BATTERY UNDER SIMULATED ELECTRIC VEHICLE DRIVING REQUIREMENTS				5. Report Date May 1981	
				6. Performing Organization Code 778-36-06	
7. Author(s) John G. Ewashinka and John M. Bozek				8. Performing Organization Report No. E-717	
9. Performing Organization Name and Address National Aeronautics and Space Administration Lewis Research Center Cleveland, Ohio 44135				10. Work Unit No.	
				11. Contract or Grant No.	
12. Sponsoring Agency Name and Address U. S. Department of Energy Office of Transportation Programs Washington, D. C. 20585				13. Type of Report and Period Covered Technical Memorandum	
				14. Sponsoring Agency Code Report No. DOE/NASA/51044-19	
15. Supplementary Notes Final report. Prepared under Interagency Agreement DE-AI01-77CS51044.					
16. Abstract A state-of-the-art 6-V battery module in current use by the electric vehicle industry was tested at the NASA Lewis Research Center to determine its performance characteristics under the SAE J227a driving schedules B, C, and D. The primary objective of the tests was to determine the effects of periods of recuperation and long and short periods of electrical regeneration in improving the performance of the battery module and hence extending the vehicle range. A secondary objective was to formulate a computer program that would predict the performance of this battery module for the above driving schedules. The results show excellent correlation between the laboratory tests and predicted results. The predicted performance compared with laboratory tests was within +2.4 to -3.7 percent for the D schedule, +0.5 to -7.1 percent for the C schedule, and better than -11.4 percent for the B schedule.					
17. Key Words (Suggested by Author(s)) Batteries Electric vehicle Computer modeling Electrochemical devices			18. Distribution Statement Unclassified - unlimited STAR Category 44 DOE Category UC-94c		
19. Security Classif. (of this report) Unclassified		20. Security Classif. (of this page) Unclassified		21. No. of Pages	22. Price*



